1,1 -Dimethyl-4,4 -bipyridinium as a multivalent structure-directing counterion to anionic uranyl ion polycarboxylate complexes

Youssef Atoini, Sotaro Kusumoto, Yoshihiro Koide, Shinya Hayami, Yang Kim, Jack Harrowfield, Pierre Thuéry

1,1′-Dimethyl-4,4′-bipyridinium as a multivalent structure-directing counterion to anionic uranyl ion polycarboxylate complexes

Youssef Atoini[a], Sotaro Kusumoto[b], Yoshihiro Koide[b], Shinya Hayami[c], Yang Kim[c,*], Jack Harrowfield[d,*], Pierre Thuéry[e,*]

[a] *Technical University of Munich, Campus Straubing, Schulgasse 22, 94315 Straubing, Germany*
[b] *Department of Material & Life Chemistry, Kanagawa University, 3-27-1 Rokkakubashi, Kanagawa-ku, Yokohama 221-8686, Japan*
[c] *Department of Chemistry, Graduate School of Science and Technology, Institute of Industrial Nanomaterials (IINa), Kumamoto University, 2-39-1 Kurokami, Chuo-ku, Kumamoto 860-8555, Japan*
[d] *Université de Strasbourg, ISIS, 8 allée Gaspard Monge, 67083 Strasbourg, France*
[e] *Université Paris-Saclay, CEA, CNRS, NIMBE, 91191 Gif-sur-Yvette, France*

* Corresponding authors.
E-mail addresses: ykim@kumamoto-u.ac.jp (Y. Kim), harrowfield@unistra.fr (J. Harrowfield), pierre.thuery@cea.fr (P. Thuéry)

Abstract

Seven uranyl ion complexes with polycarboxylates have been synthesized under solvo-hydrothermal conditions and in the presence of 1,1′-dimethyl-4,4′-bipyridinium (Me_2bipy^{2+}) as structure-directing counterion. Two complexes were obtained with phthalate (pht^{2-}), $[Me_2bipy]_2[(UO_2)_4(pht)_4(O)_2]$ (**1**), which is a discrete, bis(μ_3-oxo-bridged) tetranuclear species, and $\{[Me_2bipy][(UO_2)_3(pht)_4(H_2O)]\}_n$ (**2**), which crystallizes as a monoperiodic coordination polymer. The complex obtained with citric acid (H_4cit), $\{[Me_2bipy][UO_2(Hcit)]_2{\cdot}H_2O\}_n$ (**3**), assumes a well-known monoperiodic form. $\{[Me_2bipy][(UO_2)_2(Hthftc)_2]\}_n$ (**4**), obtained from tetrahydrofurantetracarboxylic acid (H_4thftc), is also a monoperiodic polymer further assembled into layers through hydrogen bonding, the packing defining channels containing columns of stacked counterions. The previously reported $\{[Me_2bipy][(UO_2)_2(tdc)_3]\}_n$ (**5**), where tdc^{2-} is 2,5-thiophenedicarboxylate, is a diperiodic **hcb** network, with the counterions crossing the hexanuclear rings. One experiment with pimelate (pim^{2-}) gave the two complexes $\{[Me_2bipy][(UO_2)_2(pim)_3]\}_n$ (**6**) and $\{[Me_2bipy][(UO_2)_4(pim)_5(DMA)_2]\}_n$ (**7**) (DMA = *N,N*-dimethylacetamide). Both **6** and **7** are diperiodic assemblies, but while **6** has the KIa topology previously found in other uranyl ion complexes with elongated dicarboxylate ligands, **7** is a very intricate and thick assembly with a packing displaying interdigitation. The weak interactions formed by the counterions are discussed through examination of Hirshfeld surfaces.

Keywords: Uranyl ion, 1,1′-Dimethyl-4,4′-bipyridinium, Metal–organic networks, Structure elucidation

1. Introduction

The affinity of uranyl ion for carboxylate donor ligands has led to the existence of a large number of anionic complexes, many, though not all, containing the $[UO_2(O_2CR)_3]^-$ entity, both in isolation or as a unit in a polymer [1–3]. In their crystalline state [2–4], such complexes must be directly associated with a countercation and in the case of uranyl ion coordination polymers and oligomers, there is extensive evidence that the nature of this countercation can have a major influence on the structure adopted by the anion, defining various prospects for applications of these materials [5–10]. While incorporation of a countercation into the actual uranyl polymer chain is a case where a major influence is to be expected, many other instances where the countercation is simply coordinated as a decorative unit on the polymer chain or where it is formally an independent species are more complicated to interpret. The range of cations that might be employed is immense but of the large number that have been investigated, only a single study concerns the simple quaternized aza-aromatic, 1,1′-dimethyl-4,4′-bipyridinium (Me_2bipy^{2+}, "paraquat" or "methyl viologen", Scheme 1) [11], and it is outnumbered by studies where protonated aza-aromatics have been employed and where their structural influence appears to involve their NH-bond donor activity [12–19], a role unavailable to their quaternized derivatives. Viologens functionalized with metal ion binding groups have been more extensively studied [20,21], but in these cases the quaternary centre is covalently attached to the coordination polymer. In the present work, extension of the use of Me_2bipy^{2+} as a countercation to anionic uranyl ion complexes of previously well-studied polycarboxylate ligands has provided evidence of the peculiar behaviour of this cation. The polycarboxylic acids used cover a wide range of geometry and flexibility, including phthalic (H_2pht), citric (H_4cit), (2*R**,3*R**,4*S**,5*S**)-tetrahydrofurantetracarboxylic (H_4thftc), 2,5-thiophenedicarboxylic (H_2tdc) and pimelic (H_2pim) acids (Scheme 1). The first cases of Me_2bipy^{2+} incorporation as a counterion in this study were obtained when using the zwitterionic dicarboxylate 4,4′-

bis(carboxylatomethyl)-4,4′-bipyridinium (bcmbp) which underwent degradation into Me_2bipy^{2+} under the conditions used, in contrast to the 4,4′-bis(2-carboxylatoethyl)-4,4′-bipyridinium congener, which has been successfully used as a coligand in uranyl ion complexes [22,23], while other cases were synthesized using $Me_2bipyCl_2$. The resulting seven complexes have been characterized by their crystal structure and, where possible, their emission spectrum in the solid state. While the room temperature crystal structure of the complex involving 2,5-thiophenedicarboxylate has previously been reported [11], we present here the low temperature structure for the sake of discussion.

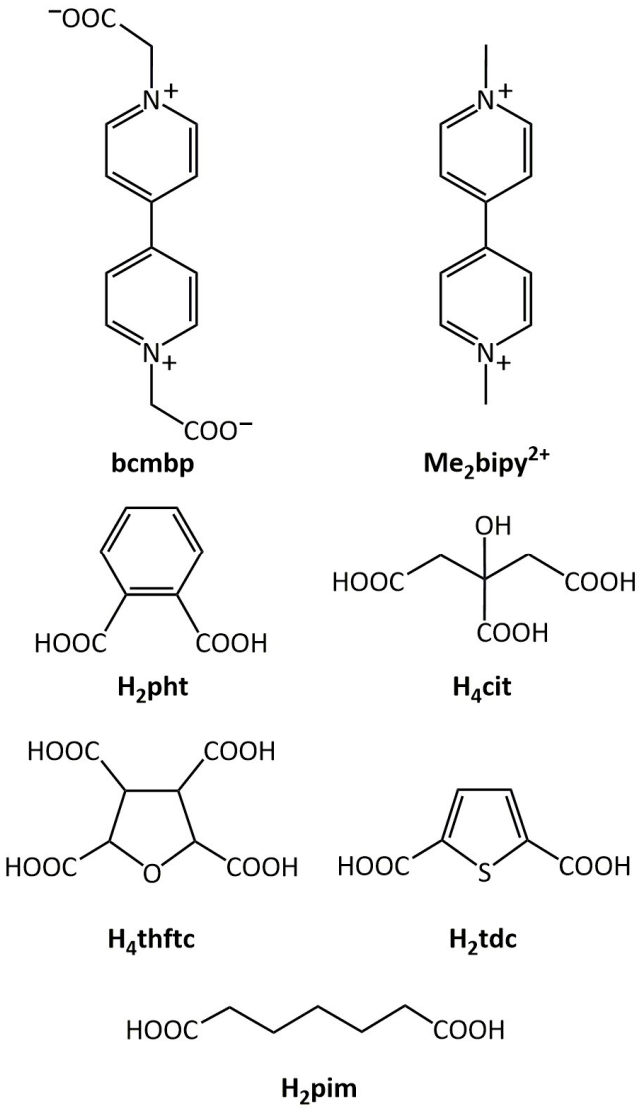

Scheme 1. The zwitterionic carboxylate bcmbp, Me_2bipy^{2+} dication, and carboxylic acids used.

2. Experimental section

2.1. Synthesis

Caution! Uranium is a radioactive and chemically toxic element, and uranium-containing samples must be handled with suitable care and protection. Small quantities of reagents and solvents were employed to minimize any potential hazards arising both from the presence of uranium and the use of pressurized vessels for the syntheses.

Dioxouranium(VI) nitrate hexahydrate, $[UO_2(NO_3)_2(H_2O)_2]\cdot 4H_2O$ (RP Normapur, 99%) was purchased from Prolabo. 1,1′-Dimethyl-4,4′-bipyridinium dichloride ($Me_2bipyCl_2$), phthalic acid (H_2pht), (2*R**,3*R**,4*S**,5*S**)-tetrahydrofurantetracarboxylic acid (H_4thftc), 2,5-thiophenedicarboxylic acid (H_2tdc) and pimelic acid (H_2pim) were from Aldrich, and citric acid (H_4cit) was from Fluka. 4,4′-Bis(hydroxycarbonylmethyl)-4,4′-bipyridinium dibromide ($bcmbpH_2Br_2$) was prepared by a slight modification of the previously reported method [24]. For all syntheses, the mixtures in demineralized water/organic cosolvent were placed in 10 mL tightly closed glass vessels and heated at 140 °C in a sand bath, under autogenous pressure. The crystals characterized were those deposited under the reaction conditions and not from subsequent cooling and depressurization.

*2.1.1. $[Me_2bipy]_2[(UO_2)_4(pht)_4(O)_2]$ (**1**)*

H_2pht (9 mg, 0.05 mmol), $[UO_2(NO_3)_2(H_2O)_2]\cdot 4H_2O$ (25 mg, 0.05 mmol), and $bcmbpH_2Br_2$ (22 mg, 0.05 mmol) were dissolved in a mixture of water (0.6 mL) and *N,N*-dimethylacetamide (DMA, 0.2 mL). A few yellow crystals of complex **1** were obtained within two weeks.

*2.1.2. $\{[Me_2bipy][(UO_2)_3(pht)_4(H_2O)]\}_n$ (**2**)*

H_2pht (17 mg, 0.10 mmol), $[UO_2(NO_3)_2(H_2O)_2]\cdot 4H_2O$ (35 mg, 0.07 mmol), and Me_2bipyCl_2 (26 mg, 0.10 mmol) were dissolved in a mixture of water (0.6 mL) and acetonitrile (0.2 mL). Yellow crystals of complex **2** were obtained within two weeks (21 mg, 54% yield based on U). *Anal.* Calc. for $C_{44}H_{32}N_2O_{23}U_3$: C, 31.63; H, 1.93; N, 1.68. Found: C, 31.98; H, 1.99; N, 2.24%.

*2.1.3. {[Me₂bipy][UO₂(Hcit)]₂·H₂O}ₙ (**3**)*

H_4cit (20 mg, 0.10 mmol), $[UO_2(NO_3)_2(H_2O)_2]\cdot 4H_2O$ (35 mg, 0.07 mmol), and Me_2bipyCl_2 (26 mg, 0.10 mmol) were dissolved in a mixture of water (0.7 mL) and DMA (0.2 mL). Yellow crystals of complex **3** were obtained within one week (24 mg, 61% yield based on U). *Anal.* Calc. for $C_{24}H_{26}N_2O_{19}U_2$: C, 25.68; H, 2.33; N, 2.50. Found: C, 25.73; H, 2.35; N, 2.72%.

*2.1.4. {[Me₂bipy][(UO₂)₂(Hthftc)₂]}ₙ (**4**)*

H_4thftc (25 mg, 0.10 mmol), $[UO_2(NO_3)_2(H_2O)_2]\cdot 4H_2O$ (35 mg, 0.07 mmol), and Me_2bipyCl_2 (26 mg, 0.10 mmol) were dissolved in a mixture of water (0.7 mL) and DMA (0.2 mL). Yellow crystals of complex **4** were obtained within one week (22 mg, 52% yield based on U). *Anal.* Calc. for $C_{28}H_{24}N_2O_{22}U_2$: C, 27.64; H, 1.99; N, 2.30. Found: C, 27.97; H, 2.01; N, 2.55%.

*2.1.5. {[Me₂bipy][(UO₂)₂(tdc)₃]}ₙ (**5**)*

H_2tdc (17 mg, 0.10 mmol), $[UO_2(NO_3)_2(H_2O)_2]\cdot 4H_2O$ (35 mg, 0.07 mmol), and Me_2bipyCl_2 (26 mg, 0.10 mmol) were dissolved in a mixture of water (0.6 mL) and acetonitrile (0.2 mL). Yellow crystals of complex **5** were obtained overnight (11 mg, 27% yield based on tdc). *Anal.* Calc. for $C_{30}H_{20}N_2O_{16}S_3U_2$: C, 29.14; H, 1.63; N, 2.27. Found: C, 29.25; H, 1.71; N, 2.52%.

*2.1.6. {[Me$_2$bipy][(UO$_2$)$_2$(pim)$_3$]}$_n$ (**6**) and {[Me$_2$bipy][(UO$_2$)$_4$(pim)$_5$(DMA)$_2$]}$_n$ (**7**)*

H_2pim (8 mg, 0.05 mmol), $[UO_2(NO_3)_2(H_2O)_2]\cdot 4H_2O$ (25 mg, 0.05 mmol), and bcmbpH_2Br_2 (22 mg, 0.05 mmol) were dissolved in a mixture of water (0.6 mL) and DMA (0.2 mL). A mixture of yellow crystals of complexes **6** and **7** was obtained within one week.

2.2. Crystallography

The data were collected at 100(2) K on a Bruker D8 Quest diffractometer equipped with an Incoatec Microfocus Source (IμS 3.0 Mo) and a PHOTON III area detector, and operated through the APEX3 software [25]. The data were processed with SAINT [26], and absorption effects were corrected for empirically with SADABS [27]. The structures were solved by intrinsic phasing with SHELXT [28] and refined by full-matrix least-squares on F^2 with SHELXL, using the ShelXle interface [29]. All non-hydrogen atoms were refined with anisotropic displacement parameters. The hydrogen atoms bound to oxygen atoms in complexes **2**, **3** and **4** were found on residual electron density maps and they were either refined with restraints or treated as riding atoms. All other hydrogen atoms were introduced at calculated positions and were treated as riding atoms with an isotropic displacement parameter equal to 1.2 times that of the parent atom (1.5 for CH_3). In **3**, one uncomplexed carboxylic group is disordered over two positions which were refined with occupancy parameters constrained to sum to unity and with restraints on bond lengths and displacement parameters. In complex **7**, the carbon chains of two pimelate ligands are partially disordered and the different positions have been refined with occupancy parameters constrained to sum to unity and with restraints on bond lengths, angles and displacement parameters. Voids in the structures of **1**, **2** and **6** are probably occupied by very disordered and unresolved solvent molecules, and the SQUEEZE software [30] was used to subtract the contribution of these solvent molecules to the structure

factors. Complex **2** crystallizes in the space group *P*1 as an inversion twin with a Flack parameter of 0.239(3); the *a* and *b* unit cell parameters of **2** are accidentally equal to one another, and the α and β angles close to each other, but no solution with a higher symmetry was found. Crystal data and structure refinement parameters are given in Table 1. Drawings were made with ORTEP-3 [31] and VESTA [32], and topological analyses were performed with ToposPro [33].

Table 1

Crystal data and structure refinement details.

	1	**2**	**3**	**4**	**5**	**6**	**7**
Chemical formula	$C_{56}H_{44}N_4O_{26}U_4$	$C_{44}H_{32}N_2O_{23}U_3$	$C_{24}H_{26}N_2O_{19}U_2$	$C_{28}H_{24}N_2O_{22}U_2$	$C_{30}H_{20}N_2O_{16}S_3U_2$	$C_{33}H_{44}N_2O_{16}U_2$	$C_{55}H_{82}N_4O_{30}U_4$
M_r	2141.07	1670.80	1122.53	1216.55	1236.72	1200.76	2231.36
Crystal system	monoclinic	triclinic	triclinic	monoclinic	monoclinic	monoclinic	triclinic
Space group	$P2_1/n$	$P1$	$P\bar{1}$	$P2_1/n$	$C2/c$	$C2/c$	$P\bar{1}$
a (Å)	13.4822(4)	13.1913(6)	8.4732(2)	5.6748(3)	12.2005(3)	19.4243(10)	12.7969(11)
b (Å)	10.6409(3)	13.1913(6)	9.8228(3)	12.4925(6)	18.0499(4)	12.3498(6)	15.9923(14)
c (Å)	20.6723(6)	14.7048(7)	19.4162(5)	22.1090(11)	15.9502(5)	18.1320(10)	19.2576(16)
α (°)	90	104.5483(17)	99.8447(9)	90	90	90	119.822(3)
β (°)	90.3327(12)	104.9745(17)	95.9368(7)	96.916(2)	102.9362(12)	113.3760(18)	91.435(3)
γ (°)	90	91.1611(18)	110.3675(8)	90	90	90	89.913(3)
V (Å^3)	2965.65(15)	2382.69(19)	1469.27(7)	1555.96(14)	3423.37(16)	3992.6(4)	3417.9(5)
Z	2	2	2	2	4	4	2
No. of reflections collected	127589	186637	28177	10334	88041	39761	42523
No. of independent reflections	9060	29058	5500	2946	8346	3779	12854
No. of observed reflections [$I > 2\sigma(I)$]	8564	28317	5376	2562	7758	3482	9890
R_{int}	0.043	0.045	0.040	0.048	0.041	0.040	0.044
No. of parameters refined	408	1314	428	245	241	241	892
R_1	0.013	0.020	0.060	0.066	0.014	0.058	0.061
wR_2	0.031	0.046	0.142	0.146	0.032	0.169	0.173
S	1.063	1.012	1.365	1.238	1.050	1.149	1.044
$\Delta\rho_{min}$ (e Å^{-3})	–0.58	–0.80	–3.40	–2.54	–0.69	–1.34	–1.10
$\Delta\rho_{max}$ (e Å^{-3})	0.83	1.39	1.90	5.28	1.07	6.18	4.23

2.3. Luminescence measurements

Emission spectra were recorded on solid samples using an Edinburgh Instruments FS5 spectrofluorimeter equipped with a 150 W CW ozone-free xenon arc lamp, dual-grating excitation and emission monochromators (2.1 nm/mm dispersion; 1200 grooves/mm) and an R928P photomultiplier detector. The powdered compounds were pressed to the wall of a quartz tube, and the measurements were performed using the right-angle mode in the SC-05 cassette. An excitation wavelength of 420 nm was used in all cases and the emission was monitored

between 450 and 600 nm. The quantum yield measurements were performed by using a Hamamatsu Quantaurus C11347 absolute photoluminescence quantum yield spectrometer and exciting the samples between 300 and 400 nm.

3. Results and discussion

3.1. Crystal structures

A dicarboxylate ligand which alone has generated a considerable volume of uranyl ion coordination chemistry is phthalate [34–44]. Amongst the quite varied complex ion species identified, a small oligomer in which four U^{VI} centres, two in pentagonal-bipyramidal and two in hexagonal-bipyramidal coordination, linked by triply-bridging oxide ions has been commonly encountered [34,35,43,44]. This same species is present in $[Me_2bipy]_2[(UO_2)_4(pht)_4(O)_2]$ (**1**), shown in Fig. 1. The tetranuclear assembly is centrosymmetric, and the U–O bond lengths are unexceptional [U–O(oxo), 1.7833(13)–1.7953(13) Å; U–O(carboxylato), 2.5543(15)–2.6079(14) Å for the κ^2O,O'-chelating groups, 2.3279(13)–2.4325(13) Å for the others; U–O(oxido), 2.2154(13)–2.2506(12) Å]. When viewed down [001], the packing displays a herringbone arrangement of tetranuclear units, with small solvent-accessible voids being present (see Experimental section), as shown by the Kitaigorodski packing index (KPI, evaluated with PLATON [45]) of 0.70. Analysis of short contacts with PLATON indicates the possible presence of two significant parallel-displaced π-stacking interactions involving both pht^{2-} ligands and the ring of the counterion containing N2 [centroid···centroid distances, 3.5996(11) and 3.7568(11) Å; dihedral angles, 3.63(9) and 10.23(9)°; slippages, 1.09 and 1.41 Å], and also one CH···π interaction between one hydrogen atom of the ring containing N2 and one pht^{2-} ring [H···centroid distance, 2.62 Å; C–H···centroid angle, 164°]. More unusual, an interaction may involve the uranyl oxo atom O1 and the ring

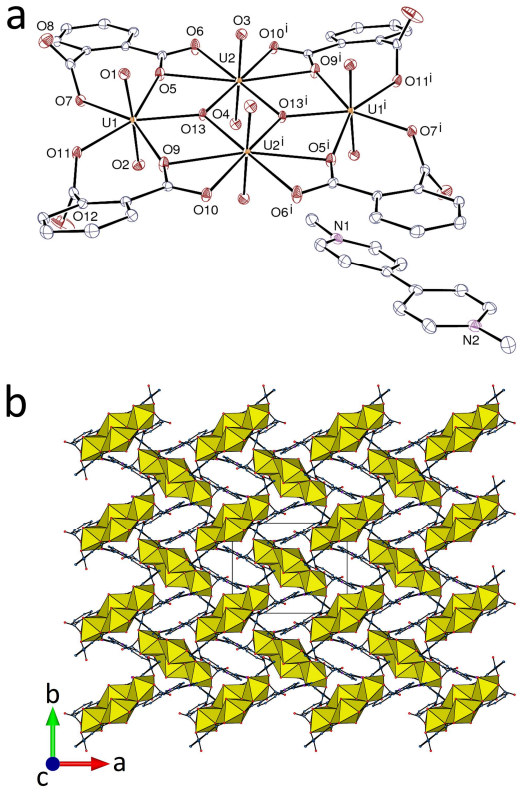

Fig. 1. (a) View of complex **1** with displacement ellipsoids shown at the 50% probability level and hydrogen atoms omitted. Symmetry code: i = 1 – *x*, 1 – *y*, 1 – *z*. (b) View of the packing with uranium coordination polyhedra colored yellow.

containing N1 [O···centroid distance, 3.2784(16) Å; U–O···centroid angle, 135.59(7)°; O1···N1 distance, 2.913(2) Å], as previously observed, for example, with pyridinium-containing zwitterionic ligands [46]. The weak interactions can be visualized through calculation of the Hirshfeld surfaces (HSs) with CrystalExplorer [47,48], with the qualification that the presence of disorder or unresolved solvent molecules introduces a degree of uncertainty which, however, should not hinder significantly the analysis of anion–cation interactions. The HS of Me_2bipy^{2+} shown in Fig. 2 clearly shows as red dots the location of the mainly lateral CH···O interactions, while the aromatic surface interactions include π-stacking interactions (white regions), an N···O=U interaction (red dot) and also several C_{arom}···O short contacts (on each face) involving carboxylate and possibly one oxo oxygen atoms, with a shorter O···C distance of 3.035(3) Å. The last interactions can be considered as an initial step of nucleophilic addition to an activated

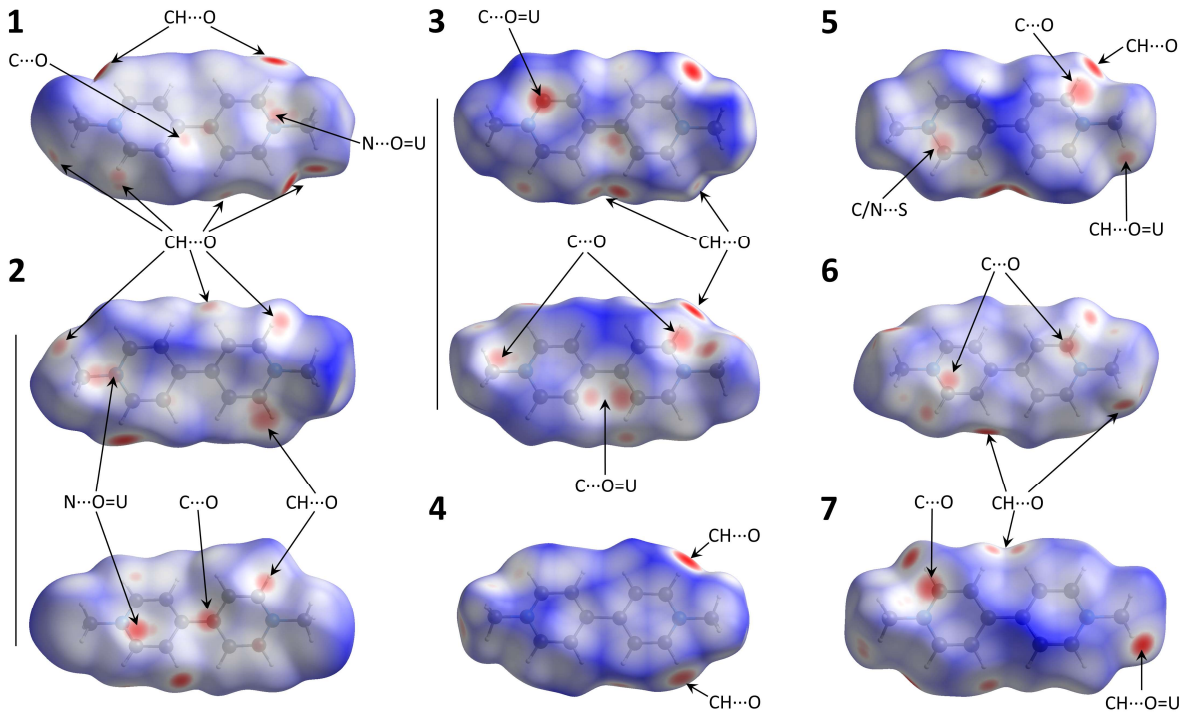

Fig. 2. Hirshfeld surfaces mapped with d_{norm} of the Me_2bipy^{2+} cations in complexes **1**–**7** with indication of the principal weak interactions formed. Not all CH···O lateral interactions are indicated for clarity. Only one HS of the two very similar counterions in **7** is shown.

double bond, a reaction type well known for its synthetic utility in, for example, functionalization of aza-aromatics activated by metal ion coordination [49]. The weak interactions in **1** involve several points of resemblance to those found previously in $[(UO_2)_4(pht)_4(O)_2Ni_2(cyclam)_2(H_2O)_2]\cdot H_2O$ (cyclam = 1,4,8,11-tetraazacyclotetradecane) where $Ni(cyclam)(H_2O)^{2+}$ can be regarded as the countercation, though here it decorates the oligomer by axial coordination to an uranyl oxo group of the pentagonal-bipyramidal centres [44]. Hydrogen bonding interactions, NH···O, OH···O and CH···O, are also evident in the structure of this complex and CH···O bonding by Me_2bipy^{2+} has been recognized as a significant influence in the known structure of $\{[Me_2bipy][(UO_2)_2(tdc)_3]\}_n$ [11], in which close approaches of coordinated oxygen to N^+ were also noted as of possible relevance to the redox activity of the solid (see ahead for further discussion of this structure). The direct contact of the

uranyl oxo group with N^+ in **1** is analogous to the axial binding of Ni^{II} to the same type of oxo group in the previous complex, although it involves only one of the N^+ centres in **1**, the other having no interaction exceeding dispersion. These different interactions of the two termini of Me_2bipy^{2+} are associated with significant twisting of the bipyridinium unit, with a dihedral angle of 16.01(8)°, though other interactions such as lateral CH···O bonding must have an influence here.

While Me_2bipy^{2+} in **1** was generated in situ from degradation of the zwitterion bcmbp, $\{[Me_2bipy][(UO_2)_3(pht)_4(H_2O)]\}_n$ (**2**) was obtained directly from $Me_2bipyCl_2$, the organic cosolvent being also changed from DMA to acetonitrile (no crystalline material having been obtained in DMA in this case). Complex **2** crystallizes in the non-centrosymmetric space group *P*1 with twice the formula content in the asymmetric unit. The six independent uranyl cations can be separated into two groups of three, with one-to-one correspondence between the two groups, both members of the couples U1/U4, U2/U5 and U3/U6 having the same environment (Fig. 3). If the counterions are disregarded, PLATON/ADDSYM indicates that the $[(UO_2)_3(pht)_4(H_2O)]_2$ motif is pseudo-centrosymmetric with 89% fit, and indeed if the U1–U3 and U4–U6 strands are considered separately, they define helices of opposite chirality, but this pseudo-symmetry is disrupted by the presence of the counterions. Atoms U1, U2, U4 and U5 are all κ^2O,O'-chelated by one carboxylate group, chelated by two carboxylate groups of another ligand to form a seven-membered ring, and bound to one more carboxylate oxygen atom from a third ligand, while U3 and U6 are κ^2O,O'-chelated by one carboxylate group and bound to two more oxygen donors from two different ligands and a water molecule, all uranium atoms being thus in pentagonal-bipyramidal environments [U–O(oxo), 1.765(4)–1.783(4) Å; U–O(carboxylato), 2.401(4)–2.477(4) Å for the κ^2O,O'-chelating groups, 2.293(4)–2.433(4) Å for the others; U–O(water), 2.409(4) and 2.395(4) Å]. All uranium atoms are 3-coordinated (3-c) nodes, while the ligands are either 3-c nodes or simple links, and the polymer formed is

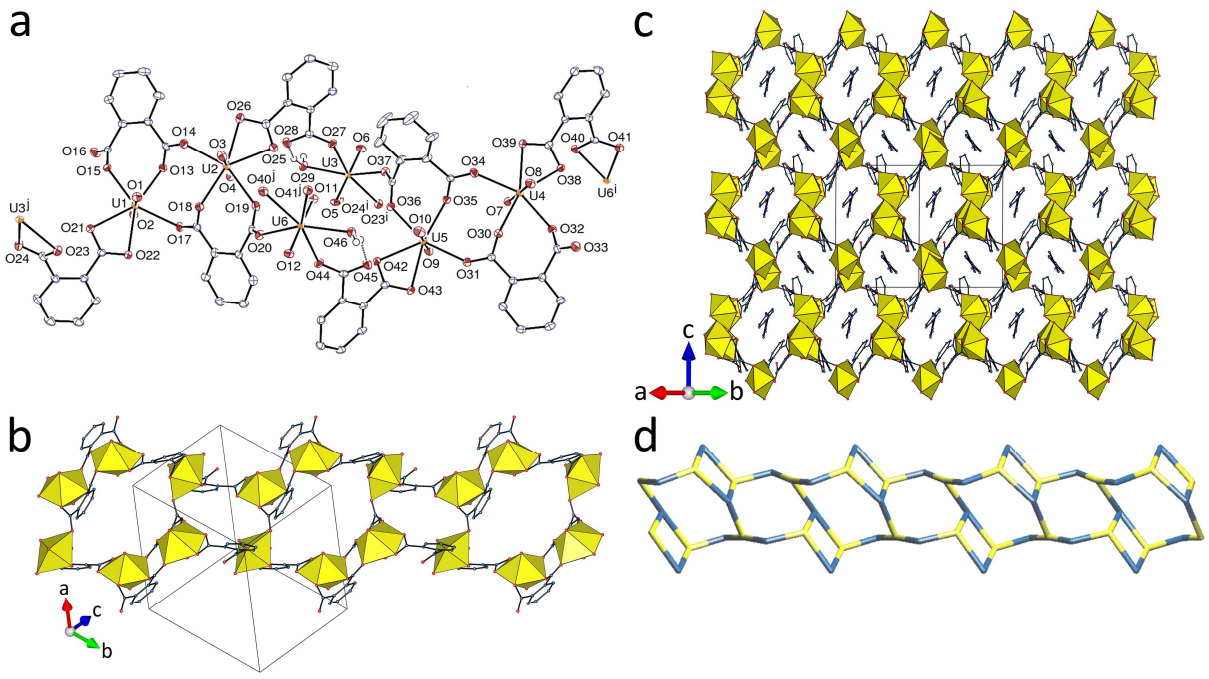

Fig. 3. (a) View of compound **2** with displacement ellipsoids shown at the 50% probability level. The counterions and carbon-bound hydrogen atoms are omitted, and hydrogen bonds are shown as dashed lines. Symmetry codes: i = *x*, *y* – 1, *z* – 1; j = *x*, *y* + 1, *z* + 1. (b) View of the monoperiodic polymer. (c) Packing viewed along the channels direction. (d) Nodal representation of the polymer (uranium nodes, yellow; pht^{2-} nodes and edges, blue).

monoperiodic and directed along [011]. The chains are built from concatenated tetranuclear rings of slightly different shape (22- or 28-membered), with simple dinuclear rings appended at their junction (Fig. 3d). When viewed down [110], the packing defines channels occupied by the counterions, with small solvent-accessible voids being present (KPI, 0.68). As in complex **1**, there is a significant twist of each of the two inequivalent Me_2bipy^{2+} units [dihedral angle for that involving N1 and N2, 18.1(3)°, for that involving N3 and N4, 26.8(3)°], with both having the same chirality, whereas in complex **1** the unique cation is present as both enantiomers. Parallel-displaced π-stacking interactions involving pht^{2-} and Me_2bipy^{2+} may be present [centroid···centroid distances, 3.864(3) and 4.106(4) Å; dihedral angles, 1.7(3) and 4.6(3)°], and also CH···π interactions between three hydrogen atoms of the counterions and pht^{2-} rings [H···centroid distances, 2.85–2.97 Å; C–H···centroid angles, 140–178°]. Here also, two

U=O···N interactions are probably significant, which involve the oxo atoms O5 and O7 and the N1 and N4 centres, respectively [O···N distances, 2.863(6) and 3.168(7) Å]. All these interactions are apparent on the HSs (Fig. 2), as well as short O···C_{arom} contacts involving carboxylate oxygen atoms, the shortest being at 2.824(7) Å.

Another ligand with a well-established uranyl ion coordination chemistry is citrate [50–54], which, in $\{[Me_2bipy][UO_2(Hcit)]_2 \cdot H_2O\}_n$ (**3**), adopts a trianionic form produced by loss of two carboxylic protons and that of the hydroxyl group. The asymmetric unit contains two separate but similar units, each with a single uranyl cation whose coordination mode is that very frequently found with this ligand, with chelation by one carboxylate and the hydroxide donor of two ligands to form one five- and one six-membered chelate rings, and further bonding to one carboxylate donor from a third ligand, giving a pentagonal-bipyramidal environment [U–O(oxo), 1.742(11)–1.819(9) Å; U–O(carboxylato), 2.332(9)–2.462(9) Å; U–O(hydroxido), 2.362(9)–2.419(9) Å] (Fig. 4). This results in formation of dimeric units $\{[UO_2(Hcit)]_2\}^{2-}$ which are doubly connected to one another to form a monoperiodic polymer of a well-known form [54], here directed along [100]. Hydrogen bonding of the carboxylic groups to oxo or carboxylato oxygen atoms of neighbouring chains [O···O, 2.614(14)–2.94(2) Å; O–H···O, 160–177°] leads to the formation of a triperiodic network, with channels parallel to [100] containing the counterions (Fig. 4c), the KPI being ~0.74. Here, the two inequivalent, planar Me_2bipy^{2+} cations are centrosymmetric. The disorder affecting one carboxylic group (see Experimental section) hinders exact calculation of the HSs (which have been generated with only one of the disordered positions affected with complete occupancy and thus gives only a rough approximation of the corresponding region), but it can be ascertained nevertheless that here also uranyl oxo groups on both uranium centres are involved in interactions with Me_2bipy^{2+} carbon atoms, if in different ways since they interact with atoms located differently in the aromatic rings (Fig. 2), with O···C distances of 2.876(17) and 2.95(2) Å.

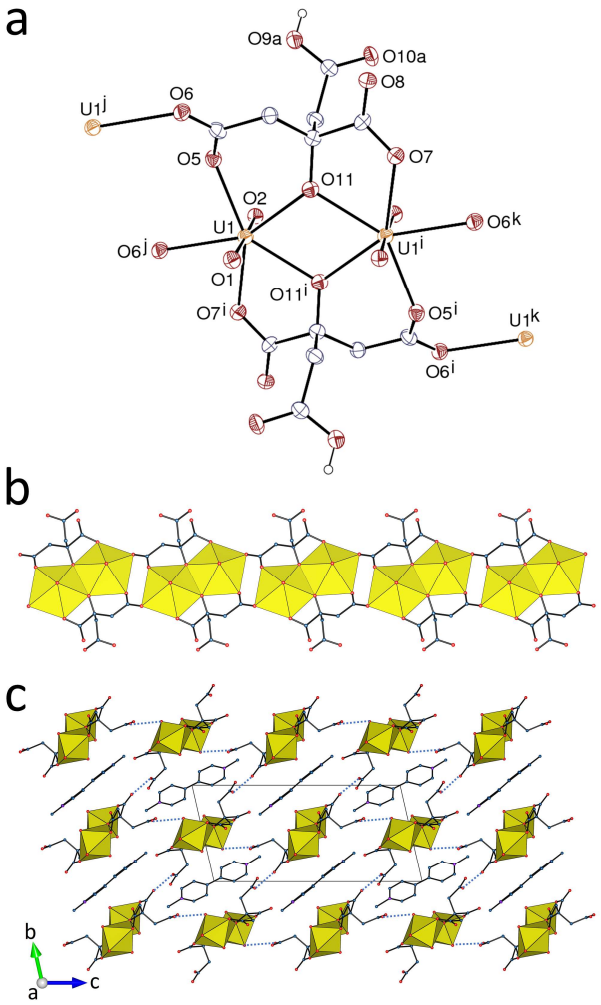

Fig. 4. (a) View of one of the two independent units in compound **3** with displacement ellipsoids shown at the 30% probability level. The counterion, solvent molecule and carbon-bound hydrogen atoms are omitted, and only one position of the disordered groups is represented. Symmetry codes: i = 1 – *x*, 1 – *y*, 1 – *z*; j = 2 – *x*, 1 – *y*, 1 – *z*; k = *x* – 1, *y*, *z*. (b) View of the monoperiodic polymer. (c) Packing viewed down the chain axis, with hydrogen bonds shown as dashed lines.

Although less frequently studied than anions derived from phthalic or citric acid, those derived from tetrahydrofurantetracarboxylic acid (H_4thftc) have given rise to uranyl ion complexes of a remarkable variety of structures [55–58], in part associated with isomerization under different preparative conditions between its (commercially available) achiral 2*R**,3*R**,4*S**,5*S** and chiral 2*R**,3*S**,4*S**,5*S** forms. In the presence of Me_2bipy^{2+}, the complex isolated has the composition $\{[Me_2bipy][(UO_2)_2(Hthftc)_2]\}_n$ (**4**) in which the $Hthftc^{3-}$ anion

retains the 2*R**,3*R**,4*S**,5*S** configuration. The single uranium atom is in a pentagonal-bipyramidal environment, being chelated by two carboxylates and the ether group of one ligand, thus forming two fused 5-membered chelate rings, and also chelated by two carboxylate groups of a second ligand so as to form a 7-membered ring [U–O(oxo), 1.709(12) and 1.773(11) Å; U–O(carboxylato), 2.286(9)–2.362(11) Å; U–O(ether), 2.574(11) Å] (Fig. 5). The resulting

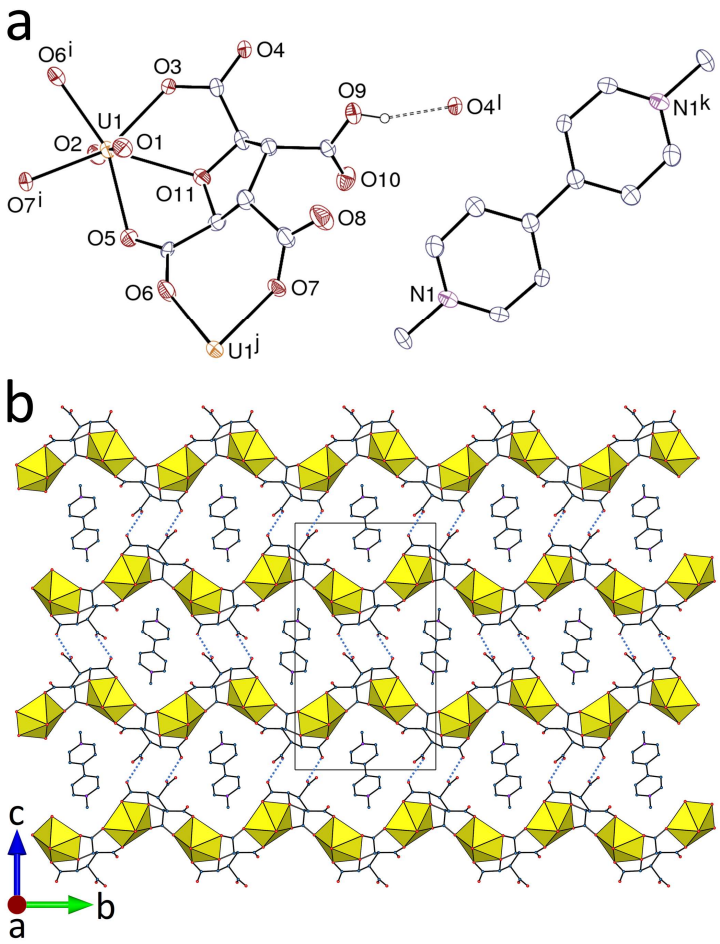

Fig. 5 (a) View of compound **4** with displacement ellipsoids shown at the 30% probability level. Carbon-bound hydrogen atoms are omitted and the hydrogen bond is shown as a dashed line. Symmetry codes: i = 3/2 – *x*, *y* – 1/2, 3/2 – *z*; j = 3/2 – *x*, *y* + 1/2, 3/2 – *z*; k = 2 – *x*, –*y* – 1, 1 – *z*; l = –*x*, 1 – *y*, 1 – *z*. (b) Packing with hydrogen bonds shown as dashed lines.

coordination polymer is monoperiodic, a form not previously observed, and directed along [010], with a simple alternation of metal ions and ligands. Reciprocal, double hydrogen bonding of carboxylic to carboxylate groups of two ligands unites the chains into diperiodic assemblies

parallel to (10–3) [O···O, 2.647(13) Å; O–H···O, 160°]. The planar, centrosymmetric counterions are located within channels parallel to [100], forming columns held by parallel-displaced π-stacking interactions [centroid···centroid distance, 3.815(9) Å; dihedral angle, 0°; slippage, 1.00 Å], the overall packing being quite compact (KPI, 0.76). Examination of the HS of the counterion (Fig. 2) shows no other prominent interaction than the lateral CH···O, with no close approach of oxo and carboxylato groups to the aromatic rings, due to the packing of counterions into columns, with at most a barely detectable C_{arom}···O=U contact of 3.147(19) Å.

Another ligand widely exploited in uranyl ion coordination chemistry is the dianion derived from 2,5-thiophenedicarboxylic acid (H_2tdc) [11,15,46,59–66]. The crystal structure of the complex $\{[Me_2bipy][(UO_2)_2(tdc)_3]\}_n$ (**5**) has previously been determined at room temperature [11], and we report only briefly here the structure determined at 100 K for the sake of discussion of weak interactions. The unique uranium atom is here tris(κ^2O,O'-chelated) by three tdc^{2-} ligands to form the common diperiodic polymer with **hcb** topology [U–O(oxo), 1.7680(10) and 1.7771(10) Å; U–O(carboxylato), 2.4441(10)–2.5202(9) Å] (Fig. 6). In addition to the usual CH···O interactions, the HS (Fig. 2) does indicate the centrosymmetric cation to be involved in two weak interactions with thiophene sulfur atoms, generally observed in other known structures not to be involved in any interaction beyond dispersion. These interactions involve only one of the two inequivalent tdc^{2-} units, that containing S1, but both ends of the cation, with a C–N bond the site of contact [N···S, 3.2745(12) Å; C···S, 3.2691(13) Å]. To the opposite face of this same bond, interactions with a carboxylate oxygen atom occur [C···O, 2.8590(16) Å; N···O, 3.1181(15) Å], while an uranyl oxo group is here involved only in hydrogen bond acceptance from a methyl group. With a KPI of 0.71, the packing does not contain solvent-accessible voids.

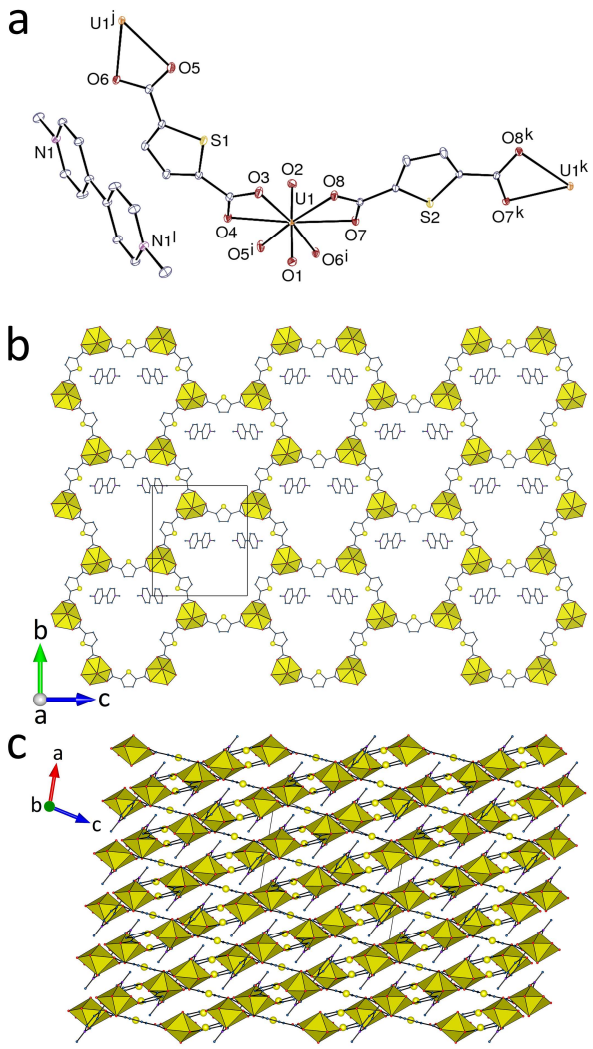

Fig. 6 (a) View of compound **5** with displacement ellipsoids shown at the 50% probability level and hydrogen atoms omitted. Symmetry codes: i = 1/2 – *x*, *y* + 1/2, 1/2 – *z*; j = 1/2 – *x*, *y* – 1/2, 1/2 – *z*; k = 1 – *x*, *y*, 3/2 – *z*; l = 1 – *x*, 1 – *y*, –*z*. (b) View of the diperiodic network and the counterions closer to the rings. (c) Packing with sheets viewed edge-on.

Aliphatic dicarboxylic acids are another well-studied source of uranyl ion ligands [12,67–72], with the C_7 species, pimelic acid (H_2pim), commonly encountered. The complex $\{[Me_2bipy][(UO_2)_2(pim)_3]\}_n$ (**6**) has the stoichiometry suited to the provision of three carboxylate units for each uranyl but it is known [67] that this does not guarantee the formation of a simple honeycomb diperiodic array, even when hexagonal-bipyramidal coordination of the U^{VI} centres is achieved, and in fact the length and flexibility of pimelate appear to enable its

complexes to adopt a variety of more complicated forms. In the present case, the unique uranium atom is tris(κ^2O,O'-chelated) by three pim^{2-} ligands [U–O(oxo), 1.783(8) and 1.790(9) Å; U–O(carboxylato), 2.443(8)–2.499(9) Å], and it is thus a 3-c node (Fig. 7). The diperiodic network formed, parallel to (001), is however not the common **hcb**, but it has the $\{8^2.10\}$ point symbol and the KIa topological type, previously found in several uranyl ion complexes with elongated ligands [12,46,70,73]. The layers are sufficiently thick (~8.5 Å) to completely encompass the counterions, which have 2-fold rotation symmetry and a dihedral angle of 20.9(2)° between the two rings. The large separation between the counterions precludes any π-stacking interaction, and the HS (Fig. 2) shows interactions of carboxylate oxygen atoms with carbon centers adjacent to N^+ only, in addition to the ubiquitous CH···O hydrogen bonds. The KPI of 0.66 indicates the presence of solvent-accessible voids.

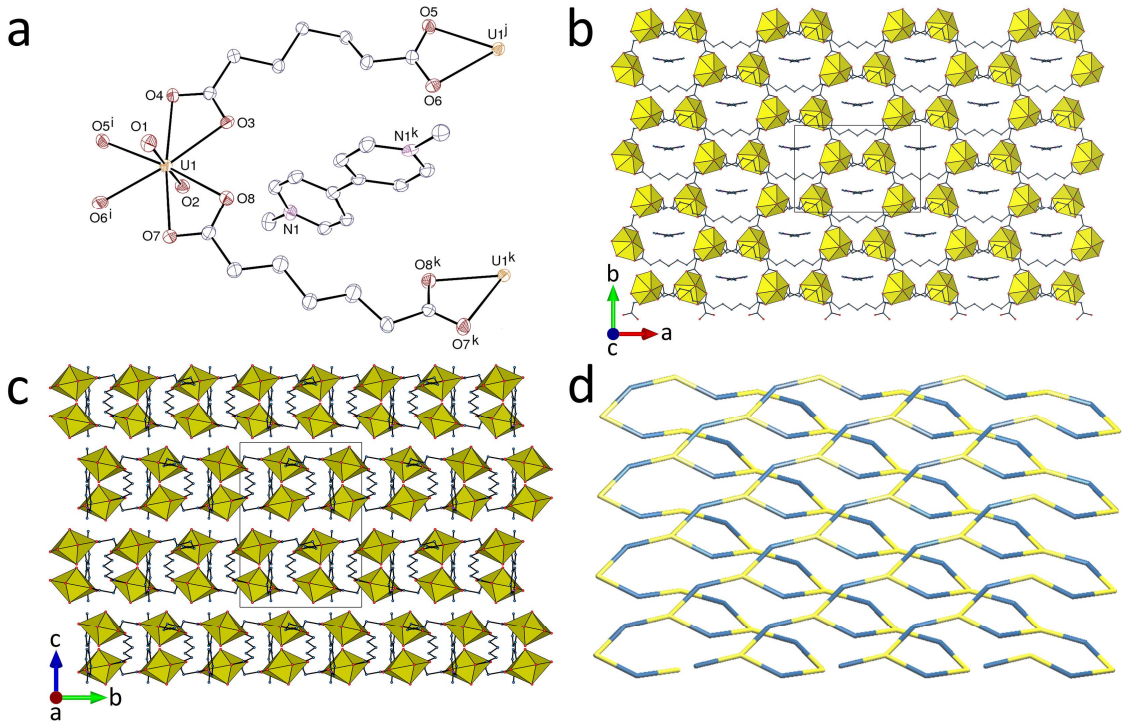

Fig. 7 (a) View of compound **6** with displacement ellipsoids shown at the 30% probability level and hydrogen atoms omitted. Symmetry codes: i = x – 1/2, y + 1/2, z; j = x + 1/2, y – 1/2, z; k = 1 – x, y, 3/2 – z. (b) View of the diperiodic network and the included counterions. (c) Packing with sheets viewed edge-on. (d) Nodal representation of the KIa network (uranium nodes, yellow; pim^{2-} edges, blue).

The versatility of pimelate as a uranyl ion ligand is further exemplified in the structure of $\{[Me_2bipy][(UO_2)_4(pim)_5(DMA)_2]\}_n$ (**7**). The asymmetric unit contains four unequivalent uranium atoms, two of them (U1 and U4) being tris(κ^2O,O'-chelated) by three pim^{2-} ligands (hexagonal-bipyramidal environment) and the other two (U2 and U3) being chelated by one pim^{2-} and bound to two more carboxylate oxygen atoms from two more ligands and one DMA molecule (pentagonal-bipyramidal environment) [U–O(oxo), 1.727(10)–1.790(9) Å; U–O(carboxylato), 2.413(9)–2.508(8) Å for the κ^2O,O'-chelating groups, 2.283(11)–2.394(8) Å for the others; U–O(DMA), 2.319(8) and 2.372(8) Å] (Fig. 8). All uranium centers are thus 3-c nodes while four pim^{2-} ligands are bis-chelating and thus simple edges, and one, partly disordered, is bis(*syn/anti*-μ_2-κ^1O:κ^1O'-bridging) and thus a 4-c node. The 3-nodal diperiodic network formed is parallel to $(01\bar{1})$ and it has the $\{10^2.12\}_2\{4.10^2\}_2\{4^2.10^4\}$ point symbol. Viewed down $[1\bar{1}\bar{1}]$ as in Fig. 8e, this complicated structure can be seen as being made up of sheets formed by side-by-side strands linking binuclear units (U2/U3) with pentagonal-bipyramidal U^{VI} centres from which project blade-like arms involving hexagonal-bipyramidal U^{VI} centres (U1/U4), the distance between outermost, limiting planes being ~23 Å. These blades of adjacent sheets interdigitate, while creating cavities accommodating the Me_2bipy^{2+} cations, placing them closer to U1 and U4 than to U2 and U3, and thus explaining contacts visible on the HS (Fig. 2) between carboxylate oxygen atoms and carbon atoms adjacent to N^+ [C···O, 2.913(13) and 3.043(15) Å for the inequivalent, planar centrosymmetric cations]. No π-stacking interaction is present, the cations being well separated from one another, and small spaces are present (KPI, 0.69).

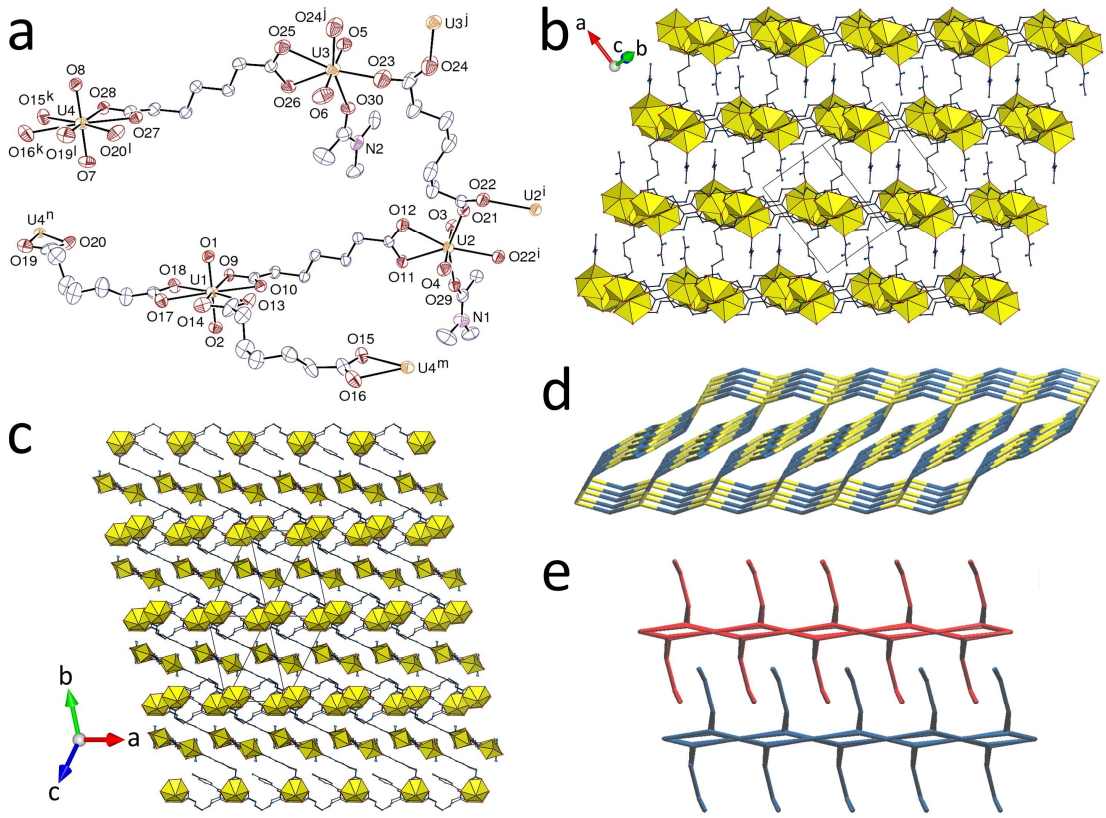

Fig. 8 (a) View of compound **7** with displacement ellipsoids shown at the 30% probability level and hydrogen atoms omitted. Only one position of the disordered parts is represented. Symmetry codes: i = –*x*, 3 – *y*, 2 – *z*; j = – *x* – 1, 2 – *y*, 1 – *z*; k = *x*, *y* – 1, *z* – 1; l = *x* – 1, *y*, *z*; m = *x*, *y* + 1, *z* + 1; n = *x* + 1, *y*, *z*; o = 2 – *x*, 1 – *y*, 1 – *z*; p = 1 – *x*, 2 – *y*, 2 – *z*. (b) View of the diperiodic network. (c) Packing with sheets viewed edge-on. (d) Nodal representation of the network (uranium nodes, yellow; pim^{2-} nodes and edges, blue). (e) Interdigitation of two layers viewed down [1$\bar{1}$1].

In all these complexes, the Me_2bipy^{2+} cation is either centrosymmetric and planar (complexes **3**, **4**, **5** and **7**), or it has 2-fold rotation symmetry or no symmetry but is very close to planar (complexes **1**, **2** and **6**), with dihedral angles between the two rings of 16.01(8)–26.8(3)°. This results in spatial separation of the continuous edge displaying the aromatic protons, with the addition of the two terminal methyl groups, and the aromatic surface. The weak interactions in which the cations are involved can thus be separated into the ubiquitous lateral and terminal CH···O hydrogen bonds, generally involving carboxylate, but also uranyl

oxo acceptors, and the aromatic interactions. Parallel-displaced π-stacking interactions are possibly present in some of the complexes only, particularly **1**, **2** and **4**, with formation of columns of counterions in the last case. In most compounds, interactions between carboxylate groups or uranyl oxo atoms and the aromatic system are discerned from the HSs (Fig. 2). In complexes **1** and **2**, they seem to involve more particularly N^+, which is close to an oxo group, while in complexes **3** and **5**–**7**, they involve carbon atoms located preferentially in ortho or meta positions with respect to nitrogen, possibly because these are sites susceptible to nucleophilic attack due to polarization of the pyridinium ring by N^+ (Scheme 2). It may be noted that interactions of oxo groups with the aromatic rings in the present series occur only in the case of pentagonal-bipyramidal uranium cations in complexes **1**–**3**, and this is true also for hydrogen bonds formed by the terminal methyl groups in **5** and **7**. These apparent distinctions in the interactions of the cation with uranyl ions having different coordination numbers may simply be a steric effect favoring the less hindered oxo groups in the pentagonal-bipyramidal species, as U=O bond lengths do not provide convincing evidence of a possible difference in basicity.

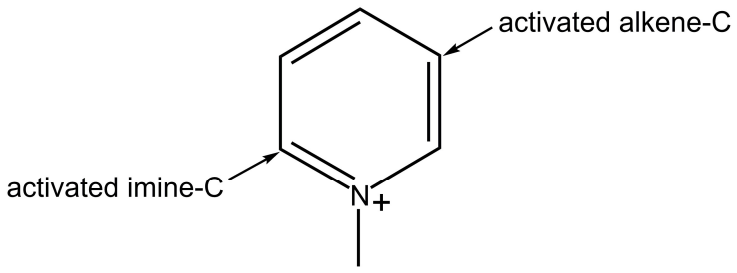

Scheme 2. Electron distribution within a pyridinium ring.

3.2. Luminescence

Emission spectra in the solid state under excitation at 420 nm were measured for complexes **2**, **3** and **4**. Complex **1** was not obtained in sufficient quantity, complexes **6** and **7** were only synthesized as a mixture, and complex **5** is non-emissive (while the previous report gave a very broad and extremely weak emission [11]), behaviour which is relatively common with

complexes of the tdc^{2-} ligand [62]. Complex **2** is the most emissive, with a photoluminescence quantum yield (PLQY) of 17%, while **3** and **4** have much smaller PLQYs of <1% and ~2%, respectively. The three spectra, shown in Fig. 9, show the typical vibronic progression due to the $S_{11} \rightarrow S_{00}$ and $S_{10} \rightarrow S_{0\nu}$ (ν = 0–4) transitions of the uranyl ion [74,75]. The four most intense peaks are located at 489, 511, 534 and 559 nm for **2**, 506, 527, 551 and 578 nm for **3**, and 496, 518, 542 and 569 nm for **4**. Uranium centres are in pentagonal-bipyramidal environments in all three complexes, and the maxima positions span the usual range for uranyl ion complexes with O_5 equatorial environments [76]. The shifts between the three spectra may be related to the slight differences in the nature of equatorial donors, five carboxylate or four carboxylate and one water oxygen atoms in **2**, three carboxylate and two alkoxide groups in **3**, and four carboxylate and one ether group in **4**. Bond valence parameters [77] calculated with PLATON [45] are consistent with this result for complexes **2** and **3** since the sums of the two bond valences for the axial donors are 3.393 and 3.183, respectively, the corresponding variation in bond strength inducing a redshift in the latter case, but not quite for **4**, in which the sum is 3.684.

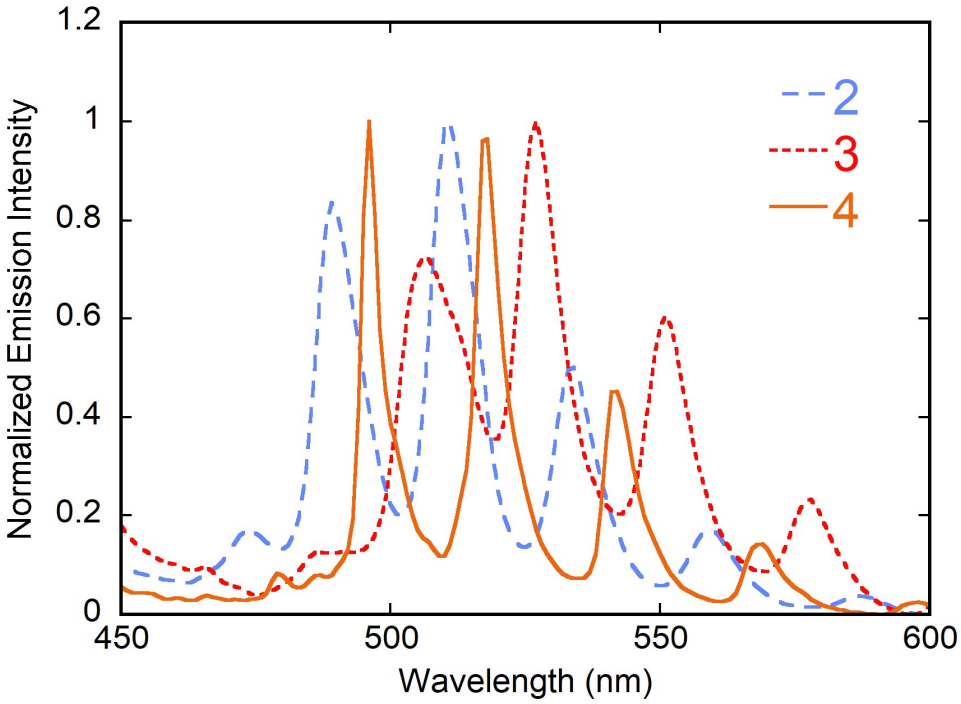

Fig. 9 Emission spectra of complexes **2**, **3** and **4** in the solid state, under excitation at 420 nm.

4. Conclusions

We have reported the synthesis and crystal structure of seven uranyl ion carboxylate complexes with Me_2bipy^{2+} as structure-directing counterion, as well as the luminescence properties for three of them. These structures involve polycarboxylates which have all been used previously in the presence of different additional reagents. The structures obtained here are only partly different in nature from those already known, since the discrete, tetranuclear complex **1** with phthalate displays a rather common geometry and coordination mode, and the monoperiodic polymer with citrate (**3**) as well as the diperiodic **hcb** network with 2,5-thiophenedicarboxylate (**5**) are also well-known motifs. The other complexes show that Me_2bipy^{2+} can in some cases give rise to new forms of anionic uranyl ion coordination polymers as a result of interactions not seen with other known cations. However, with respect to other counterions which are strong hydrogen bond donors, such as NH_4^+ or $Co(en)_3^{3+}$ (en = ethylenediamine), or which easily interact with one another such as PPh_4^+ through phenyl embrace, the interactions involving Me_2bipy^{2+} are multiple and weak and there is no obvious tendency to aggregate, somewhat limiting the structure-directing capacity of this cation.

Appendix A. Supplementary data

CCDC 2306528–2306534 contain the supplementary crystallographic data for **1**–**7**. These data can be obtained free of charge via http://www.ccdc.cam.ac.uk/conts/retrieving.html, or from the Cambridge Crystallographic Data Centre, 12 Union Road, Cambridge CB2 1EZ, UK; fax: (+44) 1223-336-033; or e-mail: deposit@ccdc.cam.ac.uk.

Declaration of Competing Interest

The authors declare that they have no known competing financial interests or personal relationships that could have appeared to influence the work reported in this paper.

References

[1] U. Casellato, P.A. Vigato, M. Vidali, Coord. Chem. Rev. 26 (1978) 85–159.

[2] J. Leciejewicz, N.W. Alcock, T.J. Kemp, Struct. Bonding 82 (2005) 43–85.

[3] P.A. Giesting, P.C. Burns, Crystallogr. Rev. 12 (2006) 205–255.

[4] T. Loiseau, I. Mihalcea, N. Henry, C. Volkringer, Coord. Chem. Rev. 266–267 (2014) 69–109.

[5] K.X. Wang, J.S. Chen, Acc. Chem. Res. 44 (2011) 531−540.

[6] M.B. Andrews, C.L. Cahill, Chem. Rev. 113 (2013) 1121−1136.

[7] J. Su, J.S. Chen, Struct. Bonding 163 (2015) 265−296.

[8] P. Thuéry, J. Harrowfield, Dalton Trans. 46 (2017) 13660−13667.

[9] J. Harrowfield, P. Thuéry, Chemistry 2 (2020) 63−79.

[10] K. Lv, S. Fichter, M. Gu, J. März, M. Schmidt, Coord. Chem. Rev. 446 (2021) 214011.

[11] H.H. Li, X.H. Zeng, H.Y. Wu, X. Jie, S.T. Zheng, Z.R. Chen, Cryst. Growth Des. 15 (2015) 10−13.

[12] L.A. Borkowski, C.L. Cahill, Cryst. Growth Des. 15 (2006) 2248−2259.

[13] M. Mirzaei, H. Eshtiagh-Hosseini, V. Lippolis, H. Aghabozorg, D. Kordestani, A. Shokrollahi, R. Aghaei, A.J. Blake, Inorg. Chim. Acta 370 (2011) 141−149.

[14] P. Thuéry, Eur. J. Inorg. Chem. (2013) 4563–4573

[15] P. Thuéry, J. Harrowfield, Cryst. Growth Des. 14 (2014) 1314−1323.

[16] P. Thuéry, J. Harrowfield, Cryst. Growth Des. 17 (2017) 2116−2130.

[17] C. Liu, C. Wang, Z.M. Sun, Inorg. Chem. 57 (2018) 15370−15378.

[18] J.F. Qian, W.J. Tian, S. Yang, Z.H. Sun, L. Chen, M.J. Wei, Z. Wu, M.Y. He, Z.H. Zhang, L. Mei, Inorg. Chem. 2020, 59, 17659−17670.

[19] Y. Zhang, X. Wang, K. Xu, F. Zhai, J. Shu, Y. Tao, J. Wang, L. Jiang, L. Yang, Y. Wang, W. Liu, J. Su, Z. Chai, S. Wang, J. Am. Chem. Soc. 145 (2023) 13161−13168.

[20] K.Q. Hu, Q.Y. Wu, L. Mei, X.L. Zhang, L. Ma, G. Song, D.Y. Chen, Y.T. Wang, Z.F. Chai, W.Q. Shi, Chem. Eur. J. 23 (2017) 18074−18083.

[21] L.W. Zeng, K.Q. Hu, L. Mei, F.Z. Li, Z.W. Huang, S.W. An, Z.F. Chai, W.Q. Shi, Inorg. Chem. 58 (2019) 14075−14084.

[22] S. Kusumoto, Y. Atoini, S. Masuda, Y. Koide, K. Chainok, Y. Kim, J. Harrowfield, P. Thuéry, Inorg. Chem. 62 (2023) 7803−7813.

[23] S. Kusumoto, Y. Atoini, Y. Koide, S. Hayami, Y. Kim, J. Harrowfield, P. Thuéry, CrystEngComm 25 (2023) 5748−5758.

[24] C. Sun, G. Xu, X.M. Jiang, G.E. Wang, P.Y. Guo, M.S. Wang, G.C. Guo, J. Am. Chem. Soc. 140 (2018) 2805−2811.

[25] APEX3, ver. 2019.1-0, Bruker AXS, Madison, WI, 2019.

[26] SAINT, ver. 8.40A, Bruker Nano, Madison, WI, 2019.

[27] (a) SADABS, ver. 2016/2, Bruker AXS, Madison, WI, 2016;
(b) L. Krause, R. Herbst-Irmer, G.M. Sheldrick, D. Stalke, J. Appl. Crystallogr. 48 (2015) 3–10.

[28] G.M. Sheldrick, Acta Crystallogr., Sect. A 71 (2015) 3–8.

[29] (a) G.M. Sheldrick, Acta Crystallogr., Sect. C 71 (2015) 3–8.
(b) C.B. Hübschle, G.M. Sheldrick, B. Dittrich, J. Appl. Crystallogr. 44 (2011) 1281–1284.

[30] A.L. Spek, Acta Crystallogr., Sect. C 71 (2015) 9–18.

[31] (a) M.N. Burnett, C.K. Johnson, ORTEPIII, Report ORNL-6895; Oak Ridge National

Laboratory: TN, 1996;

(b) L.J. Farrugia, J. Appl. Crystallogr. 45 (2012) 849–854.

[32] K. Momma, F. Izumi, J. Appl. Crystallogr. 44 (2011) 1272–1276.

[33] V.A. Blatov, A.P. Shevchenko, D.M. Proserpio, Cryst. Growth Des. 14 (2014) 3576–3586.

[34] I.A. Charushnikova, N.N. Krot, I.N. Polyakova, V.I. Makarenkov, Radiochemistry 47 (2005) 241−246.

[35] I. Mihalcea, N. Henry, T. Loiseau, Cryst. Growth Des. 11 (2011) 1940−1947.

[36] I. Mihalcea, C. Volkringer, N. Henry, T. Loiseau, Inorg. Chem. 51 (2012) 9610−9618.

[37] J. Olchowka, C. Falaise, C. Volkringer, N. Henry, T. Loiseau, Chem. Eur. J. 19 (2013) 2012−2022.

[38] A.T. Kerr, S.A. Kumalah, K.T. Holman, R.J. Butcher, C.L. Cahill, J. Inorg. Organomet. Polym. Mater. 24 (2014) 128−136.

[39] X. Gao, C. Wang, Z.F. Shi, J. Song, F.Y. Bai, J.X. Wang, Y.H. Xing, Dalton Trans. 44 (2015) 11562−11571.

[40] X. Gao, J. Song, L.X. Sun, Y.H. Xing, F.Y. Bai, Z. Shi, New J. Chem. 40 (2016) 6077−6085.

[41] W. Xu, Z.X. Si, M. Xie, L.X. Zhou, Y.Q. Zheng, Cryst. Growth Des. 17 (2017) 2147−2157.

[42] L.W. Zeng, K.Q. Hu, L. Mei, F.Z. Li, Z.W. Huang, S.W. An, Z.F. Chai, W.Q. Shi, Inorg. Chem. 58 (2019) 14075−14084.

[43] G. Andreev, N. Budantseva, A. Levtsova, M. Sokolova, A. Fedoseev, CrystEngComm 22 (2020) 8394−8404.

[44] P. Thuéry, J. Harrowfield, Cryst. Growth Des. 21 (2021) 3000–3013.

[45] A. L. Spek, Acta Crystallogr., Sect. D 65 (2009) 148–155.

[46] P. Thuéry, J. Harrowfield, Inorg. Chem. 61 (2022) 9725–9745.

[47] S.K. Wolff, D.J. Grimwood, J.J. McKinnon, M.J. Turner, D. Jayatilaka, M.A. Spackman, *CrystalExplorer*, University of Western Australia (2012).

[48] P.R. Spackman, M.J. Turner, J.J. McKinnon, S.K. Wolff, D.J. Grimwood, D. Jayatilaka, M.A. Spackman, J. Appl. Cryst. 54 (2021) 1006–1011.

[49] R. Arévalo, M.I. Menéndez, R. Lopez, I. Merino, L. Riera, J. Pérez, Chem. Eur. J. 22 (2016) 17972–17975.

[50] P. Thuéry, Chem. Commun. (2006) 853–855.

[51] J. Lhoste, N. Henry, P. Roussel, T. Loiseau, F. Abraham, Dalton Trans. 40 (2011) 2422–2424.

[52] M. Basile, D.K. Unruh, E. Flores, A. Johns, T.Z. Forbes, Dalton Trans. 44 (2015) 2597–2605.

[53] M. Basile, D.K. Unruh, K. Gojdas, E. Flores, L. Streicher, T.Z. Forbes, Chem. Commun. 51 (2015) 5306–5309.

[54] P. Thuéry, J. Harrowfield, Eur. J. Inorg. Chem. (2018) 1016–1027.

[55] P. Thuéry, C. Villiers, J. Jaud, M. Ephritikhine, B. Masci, J. Am. Chem. Soc. 126 (2004) 6838–6839.

[56] P. Thuéry, CrystEngComm 15 (2013) 6533–6545.

[57] P. Thuéry, J. Harrowfield, Cryst. Growth Des. 16 (2016) 7083–7093.

[58] P. Thuéry, J. Harrowfield, J. Coord. Chem. 76 (2023) 20–27.

[59] S.G. Thangavelu, M.B. Andrews, S.J.A. Pope, C.L. Cahill, Inorg. Chem. 52 (2013) 2060−2069.

[60] S.G. Thangavelu, R.J. Butcher, C.L. Cahill, Cryst. Growth Des. 15 (2015) 3481−3492.

[61] S.G. Thangavelu, S.J.A. Pope, C.L. Cahill, CrystEngComm 17 (2015) 6236−6247.

[62] P. Thuéry, J. Harrowfield, CrystEngComm 18 (2016) 1550−1562.

[63] S.J. Jennifer, A.K. Jana, Cryst.Growth Des. 17 (2017) 5318−5329.

[64] P. Thuéry, J. Harrowfield, Inorg. Chem. 60 (2021) 9074–9083.

[65] P.P. He, Q.Y. Xu, S.H. Li, S.M. Wei, H.H. Li, CrystEngComm 24 (2022) 3556−3564.

[66] S. Kusumoto, Y. Atoini, S. Masuda, Y. Koide, J.Y. Kim, S. Hayami, Y. Kim, J. Harrowfield, P. Thuéry, CrystEngComm 24 (2022) 7833−7844.

[67] P. Thuéry, J. Harrowfield, Inorg. Chem. 55 (2016) 2133−2145.

[68] P. Thuéry, E. Rivière, J. Harrowfield, Cryst. Growth Des. 16 (2016) 2826−2835.

[69] P. Thuéry, J. Harrowfield, Cryst. Growth Des. 17 (2017) 2116−2130.

[70] P. Thuéry, J. Harrowfield, Dalton Trans. 46 (2017) 13677−13680.

[71] P. Thuéry, Y. Atoini, J. Harrowfield, Inorg. Chem. 58 (2019) 567−580.

[72] P. Thuéry, J. Harrowfield, Inorg. Chem. 61 (2022) 2790−2803.

[73] J. Harrowfield, Y. Atoini, P. Thuéry, CrystEngComm 24 (2022) 1475–1484.

[74] A. Brachmann, G. Geipel, G. Bernhard, H. Nitsche, Radiochim. Acta 90 (2002) 147–153.

[75] M. Demnitz, S. Hilpmann, H. Lösch, F. Bok, R. Steudtner, M. Patzschke, T. Stumpf, N. Huittinen, Dalton Trans. 49 (2020) 7109–7122.

[76] P. Thuéry, J. Harrowfield, Inorg. Chem. 56 (2017) 13464–13481.

[77] N.E. Brese, M. O'Keeffe, Acta Crystallogr., Sect. B 47 (1991) 192–197.

Table of Contents Entry

1,1′-Dimethyl-4,4′-bipyridinium as a multivalent structure-directing counterion to anionic uranyl ion polycarboxylate complexes

Youssef Atoini, Sotaro Kusumoto, Yoshihiro Koide, Shinya Hayami,
Yang Kim, Jack Harrowfield, Pierre Thuéry

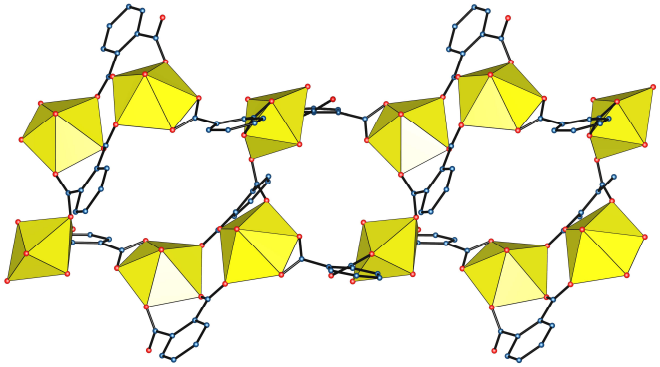

1,1′-Dimethyl-4,4′-bipyridinium (“paraquat”) was used as a structure-directing counterion in the solvo-hydrothermal synthesis of seven uranyl ion complexes with polycarboxylates, resulting in some novel arrangements and allowing an analysis of the weak interactions involved.